Journal of Biomechanics 47 (2014) 3584–3589

Contents lists available at ScienceDirect

Journal of Biomechanics

journal homepage: www.elsevier.com/locate/jbiomech
www.JBiomech.com

Short communication

Cyclic cryopreservation affects the nanoscale material properties of trabecular bone

Alexander K. Landauer [a], Sumona Mondal [b], Philip A. Yuya [a], Laurel Kuxhaus [a,*]

[a] Department of Mechanical & Aeronautical Engineering, Clarkson University, Potsdam, NY, United States
[b] Department of Mathematics, Clarkson University, Potsdam, NY, United States

ARTICLE INFO

Article history:
Accepted 30 August 2014

Keywords:
Cancellous bone
Freeze-thaw
Mechanical properties
Biomechanics
Nanoindentation

ABSTRACT

Tissues such as bone are often stored via freezing, or cryopreservation. During an experimental protocol, bone may be frozen and thawed a number of times. For whole bone, the mechanical properties (strength and modulus) do not significantly change throughout five freeze-thaw cycles. Material properties at the trabecular and lamellar scales are distinct from whole bone properties, thus the impact of freeze-thaw cycling at this scale is unknown. To address this, the effect of repeated freezing on viscoelastic material properties of trabecular bone was quantified via dynamic nanoindentation. Vertebrae from five cervine spines (1.5-year-old, male) were semi-randomly assigned, three-to-a-cycle, to 0–10 freeze-thaw cycles. After freeze-thaw cycling, the vertebrae were dissected, prepared and tested. ANOVA (factors cycle, frequency, and donor) on storage modulus, loss modulus, and loss tangent, were conducted. Results revealed significant changes between cycles for all material properties for most cycles, no significant difference across most of the dynamic range, and significant differences between some donors. Regression analysis showed a moderate positive correlation between cycles and material property for loss modulus and loss tangent, and weak negative correlation for storage modulus, all correlations were significant. These results indicate that not only is elasticity unpredictably altered, but also that damping and viscoelasticity tend to increase with additional freeze-thaw cycling.

1. Introduction

Bone tissue is frequently used in research studies. Many laboratories store bone specimens via freezing, often at the −18 °C to −20 °C range typical of industrial freezers (Langton and Njeh, 2004; Repositories, 2005). These specimens frequently undergo more than one freeze. The effect of freezing on bone material properties has been previously investigated (Borchers et al., 1995; Jung et al., 2011; Linde and Sørensen, 1993; Moreno and Forriol, 2002; Reikerås et al., 2010; Shaw et al., 2012) and has shown that changes in properties after a single freeze are not statistically significant in whole bone or cancellous bone cores. Whether additional freezing and thawing alters the tissue is unclear: a significant decrease in material properties subsequent to freeze-thaw cycling has been reported (Boutros et al., 2000; McElderry et al., 2011), while others have indicated insignificant changes (Borchers et al., 1995; Jung et al., 2011; Linde and Sørensen, 1993). Previous studies on freeze-thawing bone have been quasi-static and at the macro-scale; thus, significant changes in small-scale properties may adversely affect results of small-scale tests (e.g. Pathak et al., 2011 or Polly et al., 2012).

Nanoindentation has been used to evaluate, material-scale characteristics of bone such as inter-trabecular variation (Giambini et al., 2012; Oyen, 2010), differences between cortical and cancellous structures (Bayraktar et al., 2004), and osteonal and lamellar differences (Faingold et al., 2012; Rho et al., 1997; Zysset et al., 1999). The micro-scale viscoelastic characteristics of bone have been measured via dynamic nanoindentation (Polly et al., 2012; Rodriguez-Florez et al., 2013; Shepherd et al., 2011), in which a contact stiffness measurement method (Asif et al., 1999) is employed to calculate the material elasticity, damping, and viscoelasticity.

Given the dependence on intrinsic variables of bone material properties (Lewis and Nyman, 2008), the fundamental differences between structural and material properties of cancellous bone (Rho et al., 1998), and the impact of freeze-thawing on soft tissue, the associated damage mechanics may change at the material scale. Thus, the purpose of this work is to quantify and compare the

* Correspondence to: Department of Mechanical & Aeronautical Engineering, 8 Clarkson Ave. Box 5725, Potsdam, NY 13676, United States. Tel.: +1 315 268 6602; fax: +1 315 268 6695.
E-mail address: lkuxhaus@clarkson.edu (L. Kuxhaus).

http://dx.doi.org/10.1016/j.jbiomech.2014.08.027
0021-9290/

material-scale viscoelastic properties of cancellous bone following 0 (fresh bone) to 10 freeze-thaw cycles, under the hypothesis that no significant change will be discernible between any two cycles.

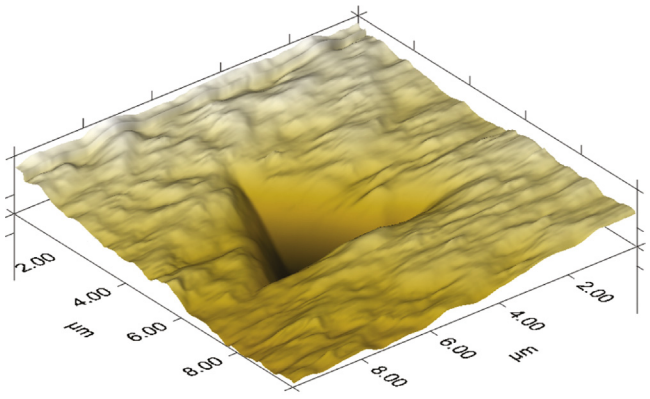

Fig. 1. Example SPM image, showing surface roughness and an indent. This region has RMS roughness of approximately 80 nm. The indent depth is much greater than the characteristic surface roughness, thus errors arising due to surface finish are likely to be small.

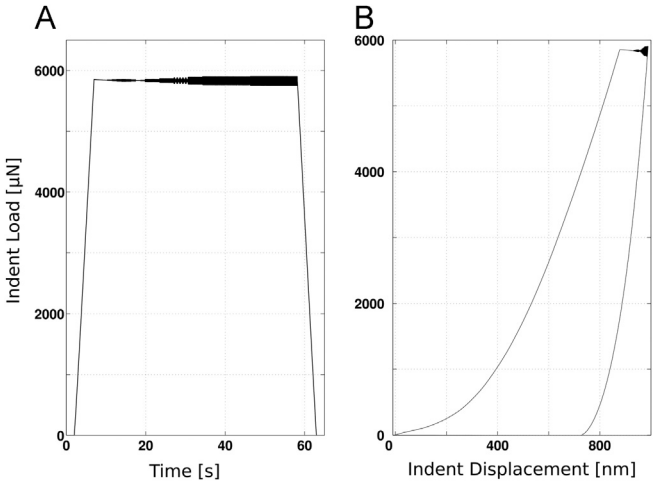

Fig. 2. (A) Load profile for indentation tests. Due to the characteristics of bone, quasi-static force was held constant across all frequencies. Although specified at 6000 μN, losses in the load column lead to slightly lower measured applied force. (B) Load–displacement curve for the same example indent. In a quasi-static analysis, the slope of the unloading curve would be used; however, with dynamic indentation, the response during the plateau period is of interest.

2. Methods

2.1. Specimen preparation

Five fresh male cervine (*Odocoileus virginianus*, white-tailed deer) spines (T2-L6 vertebrae, aged ~1.5 years as estimated by the meat processor) were obtained locally (Nolt's Custom Meat Cutting, Lowville, NY, and Twiss' Custom Meat Cutting, Potsdam, NY). All were immediately dissected into single vertebra sections. Three vertebrae were randomly selected from one spine ("donor A") and promptly prepared for nanoindentation. Vertebrae from another spine ("donor B") were then randomly assigned to cycles 1 through 3 (three vertebrae each) and frozen. For the remaining three spines ("donors C–E"), one vertebra from each was randomly assigned to a cycle from 4 to 10 and frozen. Random assignments were made via a MATLAB (The MathWorks Inc., Natick, MA) script.

For each freeze-thaw cycle, three vertebrae were frozen at −18 °C for eight or more hours and thawed at 21 °C for 6 h. After freezing and thawing a set of whole vertebrae appropriately, a cuboid of approximately 0.5 cm^3 of cancellous bone was excised from the anterior right dorsal portion of each vertebral body with an oscillating saw (Multi-Max 8300, Dremel, Waterloo, IA). In a standard preparation procedure (Dall'Ara et al., 2012; Gan et al., 2010; Giambini et al., 2012; Rho et al., 1997; Zysset et al., 1999), specimens were cleaned in an ultrasonic bath (Branson 5210, Branson Ultrasonics; Danbury CT), dehydrated in a series of alcohol baths followed by air dying, and embedded in low-viscosity epoxy (EpoxySet, Allied High Tech Inc., Rancho Dominguez, CA). The embedded specimens were polished with five grades of silicon carbide paper (320–1200 grit) and two grades of polishing slurry (1 μm diamond and 0.05 μm alumina–silica) (Allied High Tech Inc., Rancho Dominguez, CA). Debris were cleaned in an ultrasonic bath. A representative area on each specimen was imaged with scanning probing microscopy (Hysitron, Minneapolis, MN) to determine surface roughness (Fig. 1). If the root mean square (RMS) roughness was greater than 125 nm the specimen was repolished.

2.2. Nanoindentation

A load-controlled dynamic testing regime was conducted (TI-950 Triboindenter, Hysitron) with 6000 μN quasi-static force and a superimposed dynamic force of 75 μN amplitude. A frequency sweep (Oyen and Cook, 2009) from 200 Hz to 90 Hz in nine equally spaced increments was conducted during the 60-s hold period (Fig. 2). A pyramidal diamond Berkovich tip (E_t=1140 GPa and ν_t=0.07) was used. The tip area was calibrated using a fused quartz calibration specimen (Oliver and Pharr, 1992).

On each cuboidal specimen, five regions of interest (ROI) were identified via the onboard optical microscope (Fig. 3). At each ROI indents were conducted on a 4×4 grid with spacing 20 μm. Thus, 80 indents were placed on each cuboidal specimen. Sample stiffness and damping were continuously calculated (TriboScan, Hysitron) based on the contact stiffness method of Eqs. (1) and (2) (Asif et al., 1999).

$$K_s(\omega)=\left|\frac{F_0}{z_0}\right|\cos(\delta)+m\omega^2-K_i \tag{1}$$

$$C_s(\omega)=\left|\frac{F_0}{z_0}\right|\frac{\sin(\delta)}{\omega}-C_i \tag{2}$$

In these equations, F_0 is force amplitude, z_0 is displacement amplitude, m is indenter tip mass, ω is excitation frequency and δ is phase shift between force amplitude and displacement amplitude. K_i and C_i are parameters of tip stiffness and damping, respectively. The storage indentation modulus and loss indentation

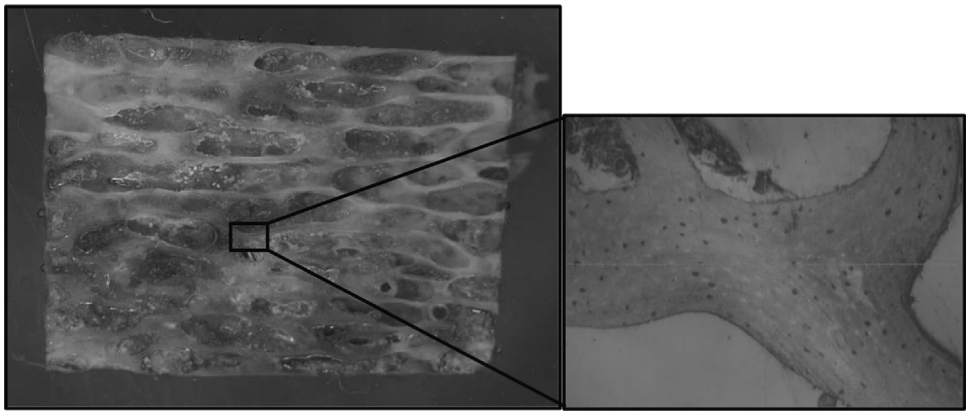

Fig. 3. Example of targeting a trabecula using on-board optical microscopy. On the left, the full surface of the cuboid is shown, imaged via digital photography. On the right, the view of a trabecula as shown via digital microscopy in the Hysitron control software is displayed; in this image the darker trabecula is seen surrounded by the lighter, more homogenous fixation epoxy.

modulus were then calculated with Eqs. (3) and (4),

$$M' = \left(\frac{K_s}{2}\right)\sqrt{\frac{\pi}{A_c}} \tag{3}$$

$$M'' = \left(\frac{\omega C_s}{2}\right)\sqrt{\frac{\pi}{A_c}} \tag{4}$$

where A_c is the tip contact area. These parameters quantify material elasticity and damping, respectively. Viscoelasticity was quantified via loss tangent, calculated with Eq. (5)

$$\tan(\delta) = \frac{M''}{M'} = \frac{\omega C_s}{K_s} \tag{5}$$

These three parameters quantify the viscoelastic response of the material (Fischer-Cripps, 2011).

2.3. Data analysis

Data processing was conducted in the Hysitron software and MATLAB, and statistical analysis in SPSS (IBM SPSS Statistics, Armonk, NY, USA). Anomalous measurements (e.g. epoxy or void strikes) were identified via a combined Studentized deleted residual test and a two standard deviation cutoff criterion, and discarded. After normality and equality of variance were verified, a univariate general ANOVA was used with factors cycle, force oscillation frequency, and donor. After establishing that unequal means existed between cycles, a Tukey's Honestly Significant Difference post-hoc multicomparison test was employed to identify significantly different means, followed by a bivariate correlation analysis using Spearman's method. This analysis was conducted individually to determine the relationship between the response variables elasticity, damping, and viscoelasticity and the predictors cycle, indentation frequency, and donor.

3. Results

3.1. Material properties

The roughness over the entire set of specimens was 103.7 ± 14.6 nm. The mean storage moduli are shown in Fig. 4(A). Although most cycles are significantly different, there is no meaningful trend in elasticity with cycle. Fig. 4(B) shows this in a plot of modulus against cycle at a single representative frequency of 105 Hz. Figs. 5 and 6 gives similar results for damping and viscoelasticity.

3.2. Statistical analysis

At $\alpha = 0.05$, the storage modulus changed significantly subsequent to most cycles. The univariate ANOVA and Tukey HSD post-hoc shows that all cycles were significantly different, except cycles 3 and 5 ($p = 1.000$) and cycles 1 and 9 ($p = 0.907$). In general, the frequency did

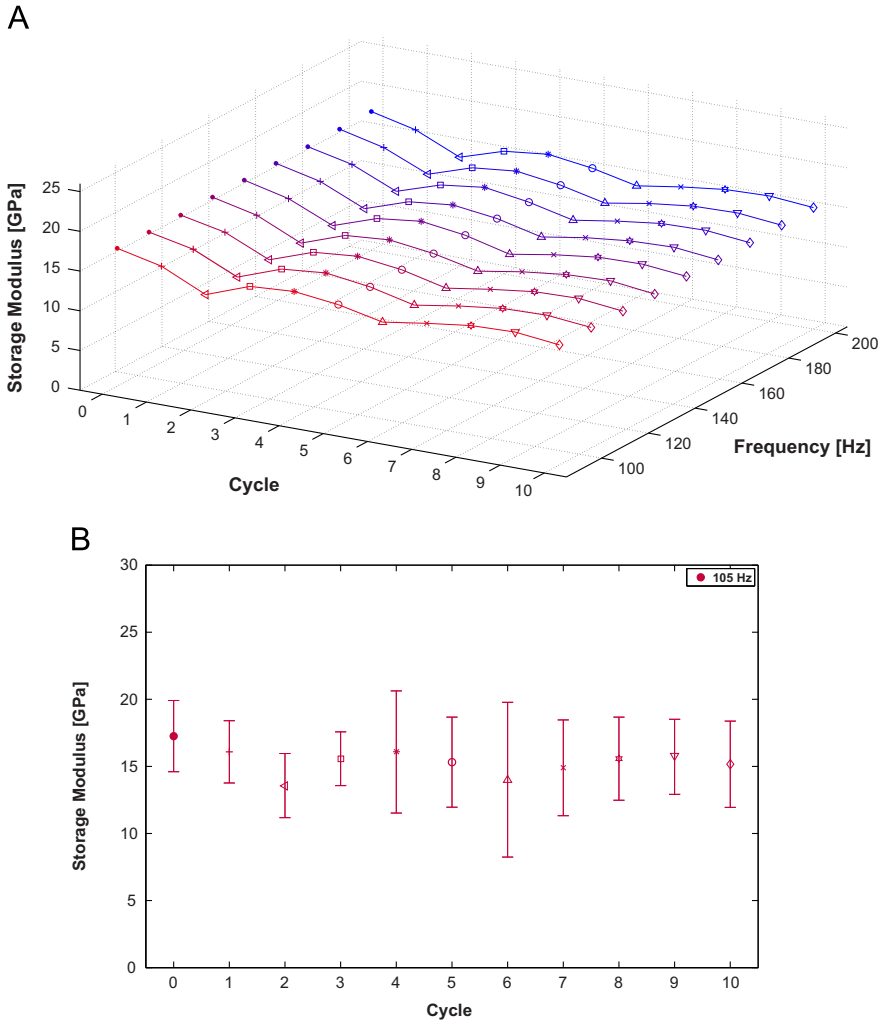

Fig. 4. (A) Storage modulus versus applied force oscillation frequency for fresh bone through 10 freeze-thaw cycles. (B) Observed storage modulus versus cycle for the 105 Hz force oscillation frequency case, with error of one standard deviation shown. In this figure, each data series represents a cycle, and color is scaled linearly from red to blue as tip force oscillation frequency scales from 90 Hz to 200 Hz. (For interpretation of the references to color in this figure legend, the reader is referred to the web version of this article.)

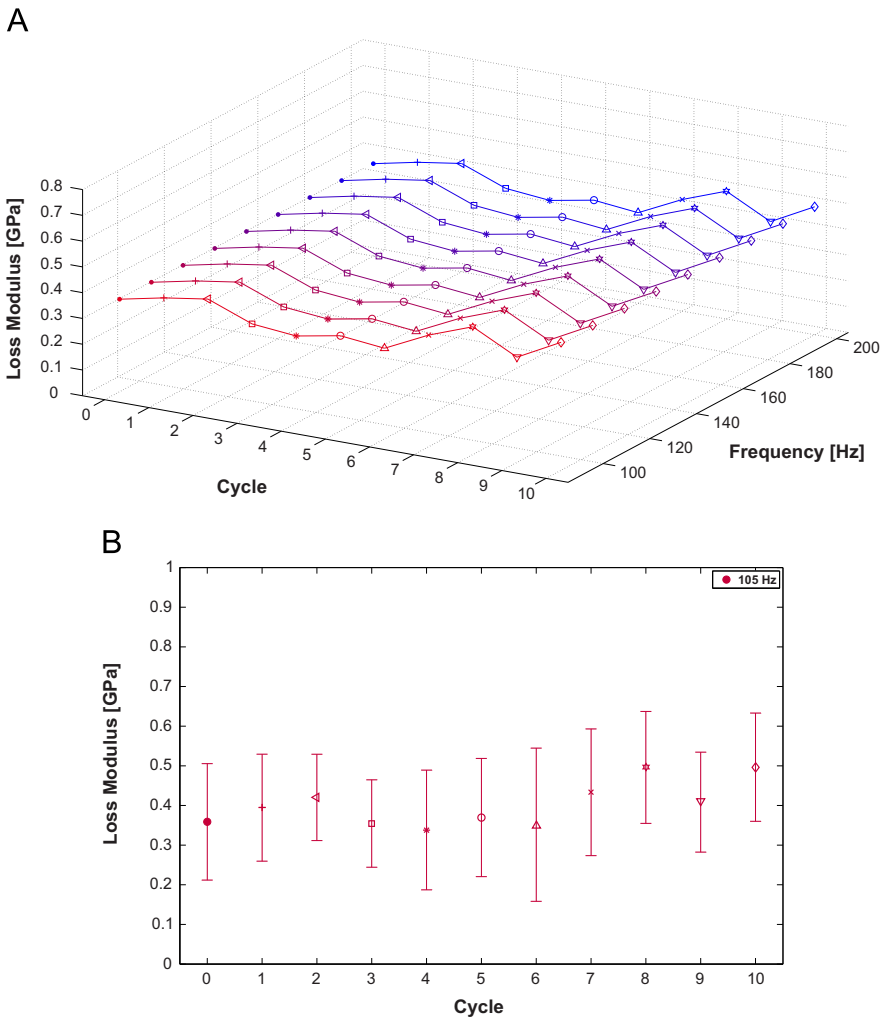

Fig. 5. (A) Loss modulus versus frequency for all cycles. (B) Loss modulus versus cycle for 105 Hz case, error bars are one standard deviation. In this figure, each data series represents a cycle, and color is scaled linearly from red to blue as tip force oscillation frequency scales from 90 Hz to 200 Hz. (For interpretation of the references to color in this figure legend, the reader is referred to the web version of this article.)

not alter the observed material elasticity, except at the 200 Hz and 186 Hz levels compared to the 90 Hz level. The storage modulus of each donor is significantly different from each other. The only significant interaction effect observed is between cycle and donor ($p<0.001$). The correlation analysis shows a small but significant ($p<0.001$) negative correlation ($r=-0.05$) between cycles and storage modulus.

Statistical tests on loss modulus showed that all cycles are different at $\alpha=0.05$, barring cycles 7 and 9 ($p=0.652$). Most frequencies are different, except the 159 Hz and 118 Hz, 118 Hz and 145 Hz, 132 Hz and 118 Hz and 90 Hz levels. Donors 2 and 4 are not significantly different from each other, but loss modulus of each other donor is significantly different from each other and from donors 2 and 4. There are no significant interaction effects. A significant ($p<0.001$) positive correlation ($r=0.205$) is found between cycles and loss modulus.

The loss tangent at each cycle is significantly different from each other cycle. Frequency has an substantial effect on loss tangent. All frequencies are significantly different, save for the 132 Hz and 105 Hz case, and the 173 Hz and 90 Hz case. For loss tangent, donors are more similar, with donors 3, 4, and 5 not significantly different from each other. There are no significant interaction effects. A significant ($p<0.001$) positive correlation ($r=0.229$) is found between the number of cycles and loss tangent.

4. Discussion

The results show that freezing and thawing has a statistically significant effect on the elastic, damping, and viscoelastic properties of cancellous bone at the small-scale. There was little trend in storage modulus with added cycles. For loss modulus and loss tangent a slight increasing trend was found, potentially linked to cumulative damage that may increase damping and viscoelasticity. The results are similar those previously reported for dehydrated bone, i.e. storage modulus ~15 GPa, loss modulus ~0.5 GPa, and loss tangent ~0.005 (Giambini et al., 2012; Isaksson et al., 2010; Polly et al., 2012). While the dehydration and drying process alters material properties, the effect of this process is not expected to change with freeze-thaw cycles (Oyen, 2010).

Bone is primarily a hydroxyapatite and Type I collagen composite, in which the properties conferred by the two materials are interrelated (Fratzl et al., 2004; Rho et al., 1998). It is unlikely that temperature variations would affect the material properties of the apatite. However, the organic collagen fibrils in calcified matter are similar to those found in soft tissue, such as ligaments and tendons (Fratzl et al., 2004), which are affected by repeated freezing and thawing (Woo et al., 1986). Thus, degradation in the collagen component is likely responsible for the observed changes. Given the intrinsic difference between structural and material scales for

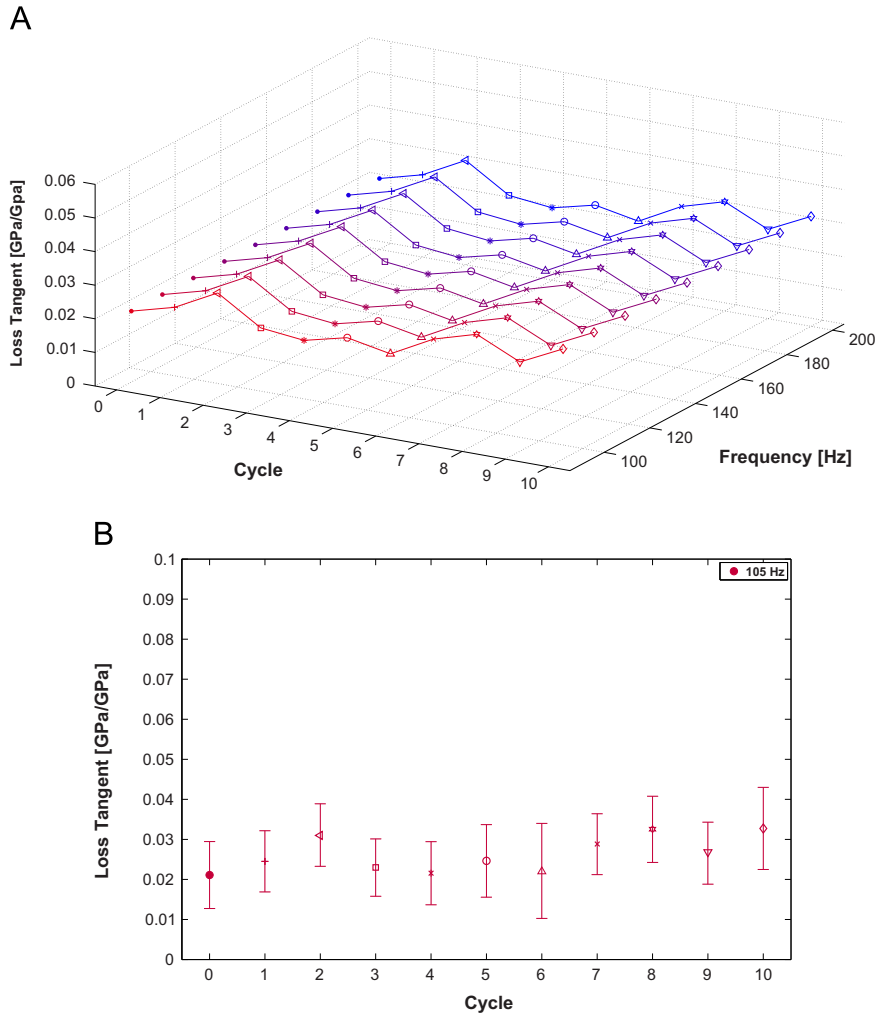

Fig. 6. (A) Loss tangent versus frequency for each cycle. (B) Loss tangent versus cycle for 105 Hz force oscillation, error bars shown are one standard deviation. In this figure, each data series represents a cycle, and color is scaled linearly from red to blue as tip force oscillation frequency scales from 90 Hz to 200 Hz. (For interpretation of the references to color in this figure legend, the reader is referred to the web version of this article.)

cancellous bone, this finding is constant with previous reports of little change at the whole bone or cancellous core scale; indeed, it may resolve a seeming disconnect between the characteristics soft-tissue collagens and calcified collagens.

Several techniques minimized error. Since the number of measurements is large (2640 indents total, 240 per cycle) with several per indent, the observed power for statistical testing is high (1.000 for all single factors). Care was taken to indent orthogonally to the primary lamellar plane, reducing variability due to anisotropy (Rho et al., 1998). At the 6000 μN load a vertical displacement of ~600 nm was obtained, limiting depth effects (Donnelly et al., 2006; Pollard, 2012). Whole vertebrae, including blood and interstitial tissue, remained intact throughout freezing and thawing, similarly typical procedures when investigating bone tissue. A primary limitation is the use of five donors. Overall change in small-scale material properties was investigated, rather than changes at specific sites or features; therefore, the results rely on bulk statistical analysis rather than directly repeated measurements. Also, with increasing freeze-thaw cycle the specimens were unfrozen for greater total time, during which biological degradation processes occurred; however, these conditions emulate those of standard preparation and testing regimes.

In conclusion, the results suggest that repeated freezing and thawing alters mechanical properties of trabecular bone. There was little trend in storage modulus. Loss modulus and loss tangent increased slightly, but significantly, as additional cycles were conducted. The statistical analysis indicates that freezing effects the tissue, which could result in unpredictable or variable measured properties at the trabecular level. Studies involving trabecular bone should be aware of this potential error source and minimize storage of specimens with cyclic cryopreservation.

Conflicts of interest statement

The authors have no conflicts of interest to report.

Acknowledgements

The authors thank Joshua Gale and Nimitt Patel for their assistance with nanoindentation. This work was partially supported by the Clarkson University Honors Program and a SEED Grant from The Coulter School of Engineering at Clarkson University.

References

Asif, S., Wahl, K., Colton, R., 1999. Nanoindentation and contact stiffness measurement using force modulation with a capacitive load–displacement transducer. Rev. Sci. Instrum. 70, 2408–2413.

Bayraktar, H.H., Morgan, E.F., Niebur, G.L., Morris, G.E., Wong, E.K., Keaveny, T.M., 2004. Comparison of the elastic and yield properties of human femoral trabecular and cortical bone tissue. J. Biomech. 37, 27–35.
Borchers, R.E., Gibson, L.J., Burchardt, H., Hayes, W.C., 1995. Effects of selected thermal variables on the mechanical properties of trabecular bone. Biomaterials 16, 545–551.
Boutros, C.P., Trout, D., Kasra, M., Grynpas, M., 2000. The effect of repeated freeze-thaw cycles on the biomechanical properties of canine cortical bone. Vet. Comp. Orthop. Traumatol. 13, 59–64.
Dall'Ara, E., Schmidt, R., Zysset, P., 2012. Microindentation can discriminate between damaged and intact human bone tissue. Bone 50, 925–929.
Donnelly, E., Baker, S.P., Boskey, A.L., van der Meulen, M.C.H., 2006. Effects of surface roughness and maximum load on the mechanical properties of cancellous bone measured by nanoindentation. J. Biomed. Mater. Res. Part A 77A, 426–435.
Faingold, A., Cohen, S.R., Wagner, H.D., 2012. Nanoindentation of osteonal bone lamellae. J. Mech. Behav. Biomed. Mater. 9, 198–206.
Fischer-Cripps, A.C., 2011. third ed Nanoindentation, vol. xxii. Springer, New York, NY p. 279.
Fratzl, P., Gupta, H., Paschalis, E., Roschger, P., 2004. Structure and mechanical quality of the collagen–mineral nano-composite in bone. J. Mater. Chem. 14, 2115–2123.
Gan, M., Samvedi, V., Cerrone, A., Dubey, D., Tomar, V., 2010. Effect of compressive straining on nanoindentation elastic modulus of trabecular bone. Exp. Mech. 50, 773–781.
Giambini, H., Wang, H., Zhao, C., Chen, Q., Nassr, A., An, K., 2012. Anterior and posterior variations in mechanical properties of human vertebrae measured by nanoindentation. J. Biomech..
Isaksson, H., Nagao, S., Małkiewicz, M., Julkunen, P., Nowak, R., Jurvelin, J.S., 2010. Precision of nanoindentation protocols for measurement of viscoelasticity in cortical and trabecular bone. J. Biomech. 43, 2410–2417.
Jung, H., Vangipuram, G., Fisher, M.B., Yang, G., Hsu, S., Bianchi, J., Ronholdt, C., Woo, S.L., 2011. The effects of multiple freeze-thaw cycles on the biomechanical properties of the human bone-patellar tendon-bone allograft. J. Orthop. Res. 29, 1193–1198.
Langton, C.M., Njeh, C.F., 2004. The Physical Measurement of Bone. IOP Publishing, Philadelphia, PA.
Lewis, G., Nyman, J.S., 2008. The use of nanoindentation for characterizing the properties of mineralized hard tissues: state-of-the art review. J. Biomed. Mater. Res. Part B Appl. Biomater. 87, 286–301.
Linde, F., Sørensen, H.C.F., 1993. The effect of different storage methods on the mechanical properties of trabecular bone. J. Biomech. 26, 1249–1252.
McElderry, J.P., Kole, M.R., Morris, M.D., 2011. Repeated freeze-thawing of bone tissue affects Raman bone quality measurements. J. Biomed. Opt. 16 (071407-071407-4).
Moreno, J., Forriol, F., 2002. Effects of preservation on the mechanical strength and chemical composition of cortical bone: an experimental study in sheep femora. Biomaterials 23, 2615–2619.
Oliver, W.C., Pharr, G.M., 1992. An improved technique for determining hardness and elastic modulus using load and displacement sensing indentation experiments. J. Mater. Res. 7, 1564.
Oyen, M.L., 2010. Handbook of Nanoindentation: With Biological Applications. Pan Stanford Publishing, Singapore.
Oyen, M.L., Cook, R.F., 2009. A practical guide for analysis of nanoindentation data. J. Mech. Behav. Biomed. Mater. 2, 396–407.
Pathak, S., Gregory Swadener, J., Kalidindi, S.R., Courtland, H., Jepsen, K.J., Goldman, H.M., 2011. Measuring the dynamic mechanical response of hydrated mouse bone by nanoindentation. J. Mech. Behav. Biomed. Mater. 4, 34–43.
Pollard, T., 2012. Dentin-Composite Interfaces: Static and Viscoelastic Properties Measured with Nanoindentation. Master's Degree Thesis.
Polly, B.J., Yuya, P.A., Akhter, M.P., Recker, R.R., Turner, J.A., 2012. Intrinsic material properties of trabecular bone by nanoindentation testing of biopsies taken from healthy women before and after menopause. Calcif. Tissue Int., 1–8.
Reikerås, O., Sigurdsen, U.W., Shegarfi, H., 2010. Impact of freezing on immunology and incorporation of bone allograft. J. Orthop. Res. 28, 1215–1219.
Repositories, E, 2005. Best practices for repositories I: Collection, storage, and retrieval of human biological materials for research. Cell Preserv. Technol., 3.
Rho, J., Kuhn-Spearing, L., Zioupos, P., 1998. Mechanical properties and the hierarchical structure of bone. Med. Eng. Phys. 20, 92–102.
Rho, J., Tsui, T.Y., Pharr, G.M., 1997. Elastic properties of human cortical and trabecular lamellar bone measured by nanoindentation. Biomaterials 18, 1325–1330.
Rodriguez-Florez, N., Oyen, M.L., Shefelbine, S.J., 2013. Insight into differences in nanoindentation properties of bone. J. Mech. Behav. Biomed. Mater. 18, 90–99.
Shaw, J.M., Boivin, G.P., Prayson, M.J., 2012. Repeated freeze-thaw cycles do not alter the biomechanical properties of fibular allograft bone. Clin. Orthop. Relat. Res. 470, 937–943.
Shepherd, T.N., Zhang, J., Ovaert, T.C., Roeder, R.K., Niebur, G.L., 2011. Direct comparison of nanoindentation and macroscopic measurements of bone viscoelasticity. J. Mech. Behav. Biomed. Mater. 4, 2055–2062.
Woo, S.L., Orlando, C.A., Camp, J.F., Akeson, W.H., 1986. Effects of postmortem storage by freezing on ligament tensile behavior. J. Biomech. 19, 399–404.
Zysset, P.K., Edward Guo, X., Edward Hoffler, C., Moore, K.E., Goldstein, S.A., 1999. Elastic modulus and hardness of cortical and trabecular bone lamellae measured by nanoindentation in the human femur. J. Biomech. 32, 1005–1012.